Inorganica Chimica Acta 498 (2019) 119175

Contents lists available at ScienceDirect

Inorganica Chimica Acta

journal homepage: www.elsevier.com/locate/ica

Research paper

Formation of a carbonato bridged Ni_4-complex by atmospheric CO_2 fixation: Crystal structure and magnetic properties

Monotosh Mondal[a,b], Júlia Mayans[c], Ashutosh Ghosh[a,*]

[a] Department of Chemistry, University College of Science, University of Calcutta, 92, A.P.C. Road, Kolkata 700 009, India
[b] Department of Chemistry, Haldia Government College, Debhog, Purba Medinipur 721657, India
[c] Departament de Química Inorgànica i Orgànica, Secció Inorgànica and Institut de Nanociència i Nanotecnologia (IN^2UB), Universitat de Barcelona, Marti i Franquès 1-11, 08028 Barcelona, Spain

ARTICLE INFO

Keywords:
Atmospheric CO_2 fixation
Tetranuclear Ni compound
New coordination mode of carbonate for Ni cluster
Magnetic interaction
Magnetostructural correlation

ABSTRACT

Reaction of $NiCl_2{\cdot}6H_2O$ with a simple N_2O donor tridentate reduced Schiff base ligand, 2-[(3-methylamino-propylamino)-methyl]-4-nitro-phenol (HL) yielded a tetranuclear complex, $[Ni_4L_4Cl_2(\mu_4\text{-}CO_3)(CH_3CN)_2]{\cdot}0.5CH_3CN{\cdot}H_2O$ (**1**) which was structurally characterized. Complex **1** is an example of atmospheric CO_2 fixation model with uniqueness in a new μ_4-κ^2:κ^2:η^1:η^1-carbonato coordination mode to Ni(II). Involvement of this type of NNO donor ligands for the synthesis of carbonato bridged polynuclear compounds by spontaneous atmospheric CO_2 fixation is very rare. All Ni(II) ions are in octahedral environment in **1** with phenoxido and hexadentate μ_4-carbonato bridging. Variable temperature magnetic measurements showed overall antiferromagnetic coupling between Ni(II) centers with $J_1 = -60.32\ cm^{-1}$, $J_2 = -19.52\ cm^{-1}$, $J_3 = 2.6\ cm^{-1}$ and $J_4 = 3.3\ cm^{-1}$. The magnetic behavior of the complex has been explained considering the carbonato and phenoxido bridging angles.

1. Introduction

Atmospheric CO_2 fixation is an important phenomenon for its relevance in controlling the global warming, usage as natural source of C1 chemical feedstock for preparation of various organic compounds by metal catalysts and conversion into metal carbonates, most of which are the useful mineral in the earth crust [1–8]. The carbonate ion is a very good and versatile flexidentate bridging ligand as each of its three oxygen atoms can coordinate to a metal ion in monodentate or bridging bidentate mode (Scheme 1) and thus can produce discrete polynuclear complexes with metal ions [9]. Such carbonate bridged complexes have drawn attention of the chemists because of their significance in understanding the bio-mineralisation process as well as the function of metalloenzymes like carbonic anhydrase and nonheme Fe(II) in the PS-II, which can activate and hydrate carbon dioxide [10–12]. Moreover, the magnetic properties of the carbonate bridged complexes of paramagnetic transition metal ions and of lanthanides are also of interest due to the intriguing magnetic coupling between the metal centers and their single molecule magnet behaviour [13–18]. However, formation of such carbonate bridged complexes by spontaneous fixation of CO_2 is rather a rare phenomenon presumably due to its low concentration in the atmosphere and high stability and therefore, the carbonate bridged complexes are prepared frequently by the addition of carbonate/bicarbonate salts or passing CO_2 to the reaction mixture [19–20]. Literature shows that spontaneous fixation occurs more often in basic solution than in neutral medium [21]. Therefore, all the reported carbonate bridged complexes produced by the spontaneous absorption of CO_2, seems to be the result of serendipity rather than planned synthesis [22–24]. A new example of such species is worthy to report as it may help in better understanding of the factors that determine its formation/isolation and consequently in designing a general method for synthesis of such complexes.

As CO_2 fixation is highly pH dependent phenomenon and usually happens in basic medium, the choice of ligands in a particular medium is one of the important factors. Various multidonating N- and/or O-donor non-Schiff base ligands are preferred for synthetic purpose because these types of ligands are resistant to any change with respect to pH of the reaction medium ($>$C=N– bond of Schiff base ligands is prone to hydrolysis at low or high pH) [25–26]. A few carbonato bridged Ni(II) complexes of Schiff base ligands are known but those Schiff bases are bi-compartmental, dinucleating types [27–29]. Involvement of simple NNO donor tridentate Schiff base ligands are very rare and only one such structure has been reported previously [30].

Hereby, we report spontaneous fixation of atmospheric CO_2 and its

---

[*] Corresponding author.
E-mail address: ghosh_59@yahoo.com (A. Ghosh).

https://doi.org/10.1016/j.ica.2019.119175
Received 22 August 2019; Received in revised form 24 September 2019; Accepted 25 September 2019

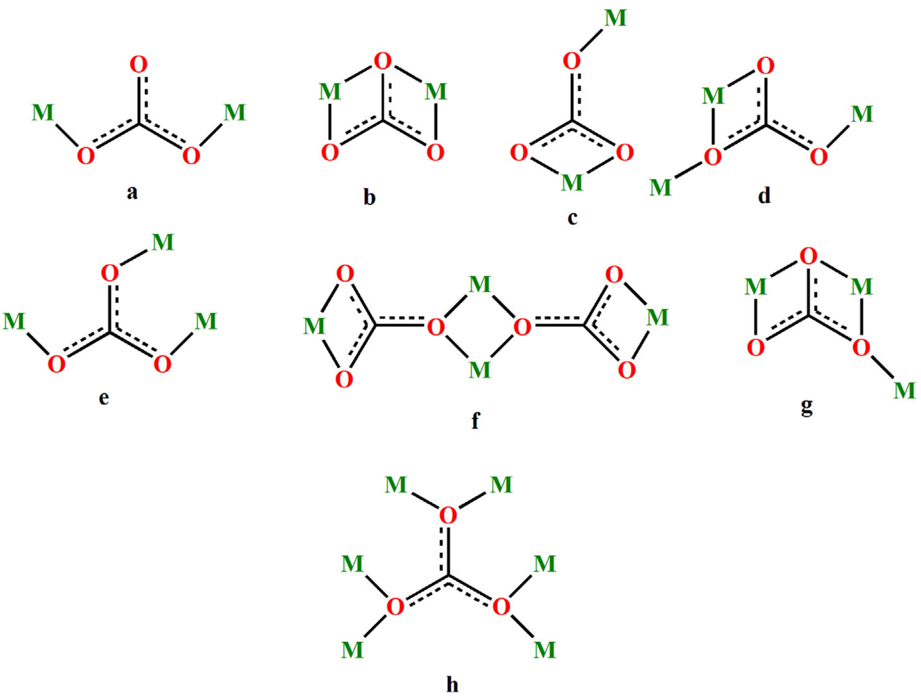

Scheme 1. Reported bridging modes of carbonate around Ni(II) centers. [a = anti-anti-μ_2, b = μ_2-κ^2:κ^2, c = μ_2-κ^2:η^1, d = μ_3-κ^2:η^1:η^1, e = syn-anti-μ_3, f = μ_4-κ^2:η^1:η^1:κ^2, g = μ_2-κ^2:κ^2:η^1, h = μ_6-η^2].

conversion into carbonate during the reaction of a NNO donor tridentate reduced Schiff bases ligand, 2-[(3-methylamino-propylamino)-methyl]-4-nitro-phenol (HL) with methanolic solution of $NiCl_2{\cdot}6H_2O$ that leads to the formation of a tetranuclear μ_4-κ^2:κ^2:η^1:η^1-carbonato bridged complex, $[Ni_4L_4Cl_2(\mu_4\text{-}CO_3)(CH_3CN)_2]{\cdot}0.5CH_3CN{\cdot}H_2O$ (**1**). The complex is separated only from basic medium and can also be synthesized by bubbling CO_2 or by addition of carbonate salt into the reaction medium. It is characterized by single crystal X-ray crystallography, electronic spectrum, IR spectrum and elemental analyses. The magnetic property of this carbonato bridged Ni_4 species is explored experimentally. The molecule is antiferromagnetically coupled, consistent with different bridging modes and angles between metals and ligands.

2. Experimental section

2.1. Starting materials

2-hydroxy-5-nitrobenzaldehyde, N-methyl-1,3-propanediamine, sodium borohydride and potassium carbonate were purchased from Spectrochem, India and were of reagent grade. They were used without further purification. The other reagents and solvents were of commercially available reagent quality, unless otherwise stated.

2.2. Synthesis of the ligand 2-[(3-methylamino-propylamino)-methyl]-4-nitro-phenol (HL)

Solid 2-hydroxy-5-nitrobenzaldehyde (835.6 mg, 5 mmol) was dissolved in warm methanol (30 mL). Then N-methyl-1,3-propanediamine (0.52 mL, 5 mmol) was added to this solution and the mixture was put under refluxed for 1 h. The resulting solution was cooled to 0 °C and solid sodium borohydride (210 mg, 6 mmol) was added slowly to it with constant stirring. After completion of the addition, the resulting mixture was acidified with concentrated HCl (5 mL) and then evaporated to dryness. The reduced Schiff-base ligand (HL) was extracted from the solid residue with methanol. This methanolic solution was used for the formation of complex [31–32].

2.3. Synthesis of $[Ni_4L_4Cl_2(\mu_4\text{-}CO_3)(CH_3CN)_2]{\cdot}0.5CH_3CN{\cdot}H_2O$ (1)

Complex **1** was produced by spontaneous atmospheric CO_2 fixation as described in method 1 below. However, the yield was low. Therefore, in order to increase the yield, method 2 (bubbling of CO_2) and method 3 (addition of K_2CO_3) were adopted.

Method 1: $NiCl_2{\cdot}6H_2O$ (518.36 mg, 4 mmol) dissolved in 20 mL of methanol, was added to a methanolic solution (20 mL) of the Schiff base (HL) (4 mmol) with constant stirring for 30 min followed by slow addition of triethylamine (0.56 mL, 4 mmol). The resulting solution was kept in open air until the solvent got evaporated to result in a solid greenish mass. The green solid was washed with diethyl ether and dissolved in CH_3CN. X-ray quality deep-green single crystals of complex **1** were obtained by diffusion of diethylether to the acetonitrile solution. These crystals were used for single crystals X-ray analysis and also for other experiments.

Yield: 288 mg; (20%). Anal. Calcd. For $C_{50}H_{73.5}Cl_2N_{14.5}Ni_4O_{16}$: C, 41.72; H, 5.15; N, 14.11. Found: C, 41.65; H, 5.05; N, 14.05. IR (KBr pellet, cm^{-1}): $\nu_{(N-H)}$, 3249 cm^{-1}, $\nu(CO_3)$, 1480, 1455, 741 cm^{-1}.

Method 2: A solution was prepared by mixing $NiCl_2{\cdot}6H_2O$ (4 mmol), HL (4 mmol) and triethylamine (4 mmol) in methanol as described above. Then CO_2 gas was bubbled through the solution for 2 h. The resulting solution was kept in open air until a greenish solid was obtained on evaporation of the solvent. The solid was dissolved in CH_3CN and layered with diethylether to obtain the crystalline product. Yield: 791.6 mg (55%) Anal. Calcd. For $C_{50}H_{73.5}Cl_2N_{14.5}Ni_4O_{16}$: C, 41.72; H, 5.15; N, 14.11. Found: C, 41.89; H, 5.21; N, 14.23.

Method 3: Solid K_2CO_3 (0.276 gm, 2 mmol) was dissolved in minimum amount of methanol-water mixture 10:1 (v/v). It was then added slowly with constant stirring to a previously synthesized solution containing $NiCl_2{\cdot}6H_2O$ (1 mmol) and ligand (1 mmol) in methanol as stated above. Slow evaporation of the resulting green solution gave a green microcrystalline compound. The green solid was then filtered and washed with diethyl ether and dissolved in CH_3CN. Crystalline product was obtained from this solution by slow diffusion of diethylether. Yield: 244.6 mg; (68%). Anal. Calcd. For $C_{50}H_{73.5}Cl_2N_{14.5}Ni_4O_{16}$: C, 41.72; H, 5.15; N, 14.11. Found: C, 41.61; H, 5.01; N, 14.00.

2.4. Physical measurements

Elemental analyses (C, H and N) were performed using a Perkin-Elmer 2400 series II elemental analyzer. An IR spectrum in KBr pellets (4500–500 cm^{-1}) was recorded using a Perkin-Elmer RXI FT-IR spectrophotometer. An Electronic spectrum (1500–250 nm) was recorded in a Hitachi U-3501 spectrophotometer. Solid-state, variable-temperature and variable-field magnetic data were collected on powdered samples using a MPMS5 Quantum Design magnetometer operating at 0.03 T in the 300 to 2.0 K range for the magnetic susceptibility and at 2.0 K in the 0–5 T range for the magnetization measurements. Diamagnetic corrections were applied to the observed susceptibilities using Pascal constants. The quality factor was parametrized as $R = (\chi_M T_{exp} - \chi_M T_{calc})^2/(\chi_M T_{exp})^2$.

2.5. X-ray crystallographic data collection and refinement

Collected diffractable single crystal of complex **1** was mounted on a Bruker-AXS SMART APEX II diffractometer equipped with a graphite monochromator and Mo-Kα ($\lambda = 0.71073$ Å) radiation. The crystal was positioned at 60 mm distance from the CCD. 360 frames were measured with a counting time of 5 s. The structure was solved using direct method by using the SHELXT 2014/5 [33]. Non-hydrogen atoms were refined with independent anisotropic thermal parameters. The hydrogen atoms bonded to carbon were included in geometric positions and given thermal parameters equivalent to 1.2 times (1.5 times for methyl hydrogens) those of the atom to which they were attached. Absorption corrections were carried out using the SADABS program [34]. The structure was refined by full-matrix least-squares on F^2 using ShelXL programme [35]. The details of crystallographic data for complex **1** are given in Table 1. CCDC-1914050 (**1**) contains the supplementary crystallographic data for this paper. These data can be obtained free of charge from The Cambridge Crystallographic Data Centre via www.ccdc.cam.ac.uk/data_request/cif (see Table 2).

3. Results and discussion

3.1. Synthesis of the complex

The tridentate Schiff base ligand was synthesized *via* condensation between N-methyl-1,3-propanediamine and 2-hydroxy-5-nitrobenzaldehyde (1:1 M ratio) in methanol. In situ reduction by sodium borohydride and subsequent treatment with conc. HCl, it readily produced the tridentate reduced ligand, 2-[(3-methylamino-propylamino)-methyl]-4-nitrophenol (HL). The ligand on reaction with $NiCl_2{\cdot}6H_2O$ in basic medium (containing triethylamine) produced tetranuclear carbonato bridged Ni(II) complex (**1**), rather serendipitously by atmospheric CO_2 fixation but in very low yield. We succeeded to produce the complex in higher yield *via* two other methods: (i) continuous bubbling of CO_2 and (ii) adding K_2CO_3 as an external source of CO_3^{2-} into the methanolic solution of $NiCl_2{\cdot}6H_2O$ and HL as described in the experimental section and shown in Scheme 2.

Table 1
Crystallographic parameters for complex **1**.

Complex	1
Chemical formula	$C_{49}H_{70}Cl_2N_{14}Ni_4O_{15}$,0.5$CH_3CN$,$H_2O$
Formula weight	1439.3
Crystal system	Tetragonal
Space group	*I*4$_1$*cd*
a(Å)	15.5680(15)
b (Å)	15.5680(15)
c (Å)	56.601(9)
α, β, γ deg	90
V (Å^3)	13718(3)
Z	4
ρ_{calc}(g cm^{-3})	1.390
μ (Mo Kα) (mm^{-1})	1.228
F(0 0 0)	5964
Reflections collected	47,815
Independent reflections	6967
Reflections with I > 2σ(I)	5516
R_1[a], wR_2[b]	0.0544, 0.1518
GOF [c]	1.02
Residual electron Density, e/Å^{-3}	−0.50, 1.54

[a] $R_1 = \Sigma||F_o| - |F_c||/\Sigma|F_o|$, [b] $wR_2\ (F_o^2) = [\Sigma[w(F_o^2 - F_c^2)^2/\Sigma w\ F_o^4]^{1/2}$ and [c] $GOF = [\Sigma[w(F_o^2 - F_c^2)^2/(N_{obs} - N_{params})]^{1/2}$.

Table 2
Hydrogen-Bond Parameters in Complex **1** (in Å and °).

D-H.......A	*d*(D-H)	*d*(D…A)	*d*(H…A)	< (D-H…A)
N(32) – H(32)…O(10)	0.98	3.054(6)	2.12	159
N(36) – H(36)…Cl(1)	0.98	3.341(5)	2.39	163
N(18) – H(18)…O(52)	0.98	3.141(13)	2.24	153

3.2. IR and electronic spectrum of the complex

The electronic spectrum (Fig. S3) of this tetranuclear Ni(II) complex are recorded in acetonitrile solution. The bands observed at 369 nm for complex **1** are assigned to those of L → M charge transfer transitions which is characteristic of the transition metal complex with Schiff base ligands. This strong band masks the higher energy *d–d* bands ($^3A_{2g} \rightarrow {}^3T_{1g}(P)$). The other two spin allowed *d-d* transitions for octahedral complex **1** (viz. $^3A_{2g} \rightarrow {}^3T_{1g}(F)$ (ν_1), $^3A_{2g} \rightarrow {}^3T_{2g}(F)$ (ν_2)) are observed at 589(ν_1) nm and at 955(ν_2) nm [36–37].

The IR spectrum (Fig. S4) of complex **1** shows a sharp peak at 3249 cm^{-1} due to the symmetric stretching vibration of N—H bond. The reduction of C═N bond is evident by absence of any sharp and strong peak at the range of 1600–1620 cm^{-1}, characteristic of C═N stretching [38–40]. According to literature survey, all carbonate related vibration modes are observed in between 1400 and 1500 cm^{-1}. The complex shows absorption peaks at 1480, 1455 and 740 cm^{-1} due to different stretching and bending modes of carbonate [41].

3.3. Description of the crystal structures

The molecular structure of complex **1** is shown in Fig. 1. It comprises of discrete tetranuclear unit of the neutral compound, $[Ni_4L_4Cl_2(\mu_4\text{-}CO_3)(CH_3CN)_2]{\cdot}0.5CH_3CN{\cdot}H_2O$ having a C_2 axis passing through the carbon (C(1)) and one of the oxygen atoms [O(2)] of carbonate ion. The asymmetric unit contains two deprotonated reduced Schiff base ligands (L^-), one chloride anion, one coordinated acetonitrile molecule, two nickel centers and half unit of bridging carbonate. In the tetrameric structure, four nickel atoms are bridged in a μ_4 fashion by a single carbonate ion *via* its oxygen atoms. The three Ni-O-Ni angles are different; thus, Ni(1)–O(1)–Ni(2) 140.5(2)°, Ni(1)–O(2)–Ni(1)[a] 175.2(4)° and Ni(2)–O(24)–Ni(2)[a] 98.2(2)° and the Ni–Ni bond distances are Ni(1)–Ni(2) 4.071 Å, Ni(1)–Ni(1)[a] 4.296 Å, and Ni(2)–Ni(2)[a] 3.157 Å. The carbonato ligand together with four Ni centers are nearly coplanar. The deviations of the Ni atoms from the mean plane passing through four Ni centers are 0.22 Å, 0.30 Å from Ni(1) and Ni(2), respectively. The average O—C—O bond angle [O(1)–C(1)–O(2), 117.5°, O(1)–C(1)–O(1)[a] , 125.0°] is 121.2°. The C—O—Ni angles are different; Ni(1)–O(1)–C(1) 89.6(5)°, Ni(2)–O(1)–C(1) 127.0(5)°, Ni(1)–O(2)–C(1) 92.4(2)°. Both the nickel atoms in the asymmetric unit are six-coordinated (Fig. S1), but the environments around them are not equivalent. Ni(1) is bonded to the uninegative chelating tridentate ligand through secondary amine nitrogen atoms, N(18), N(22) and phenoxido oxygen atom, O(10) in *mer*-configuration with usual bond distances. Two oxygen atoms [O(1), O(2)] from the central carbonate anion, and a chloride ion which is *trans* to the carbonate oxygen atom, O(2) complete the octahedral geometry. The basal plane around Ni(1)

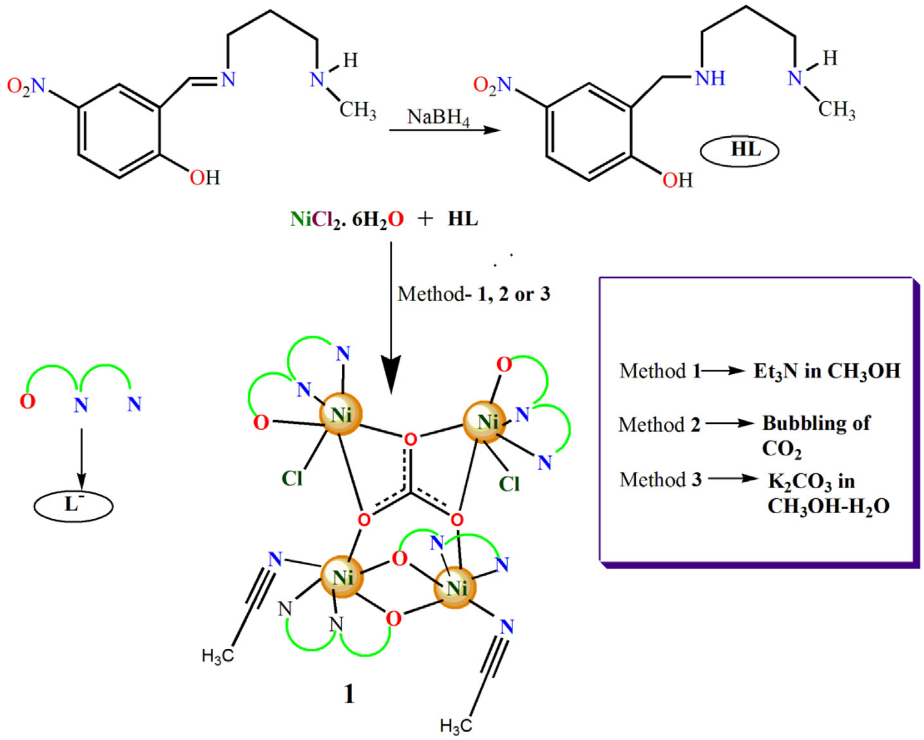

Scheme 2. Synthesis of complex **1**.

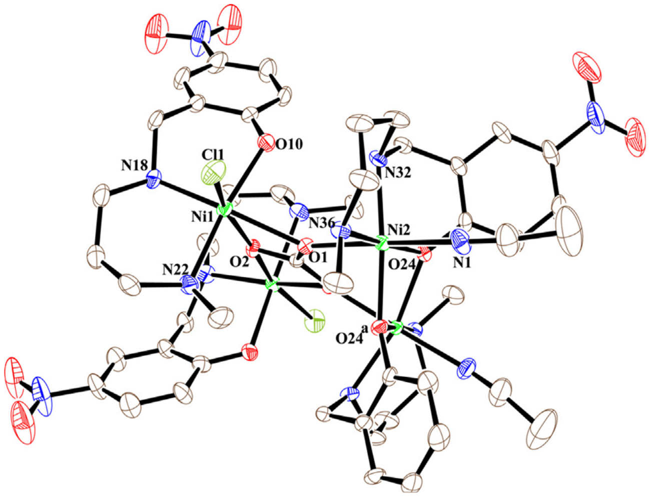

Fig. 1. Ortep diagram of complex **1** with ellipsoids at 30% probability ($^a = x, -y, -z$). Hydrogen atoms and non coordinated solvents are omitted for clarity.

center is composed of four donor atoms, N(18), Cl(1), O(2), O(1). The bond lengths in the basal plane vary in the range of 2.079(7) to 2.356(2) Å. Deviations of the coordinating atoms N(18), Cl(1), O(2) and O(1) from the least squares mean plane through them are 0.047(8), −0.042(3), −0.070(1) and −0.064(5) Å, respectively, and that of the Ni(1) atom from the same plane is 0.026(1) Å towards the axially coordinated N(22) atom. The two axial positions are occupied by O(10) and N(22) of the tridentate Schiff base at a distance of 2.062(6) and 2.139(6) Å, respectively with a O(10)–Ni(1)–N(22) bond angle of 172.2(3)°.

By contrast around Ni(2), there is no chloride anion; instead one acetonitrile solvent is coordinated to it. The hexacordination around Ni (2) is completed by the tridentate ligand in facial configuration *via* its secondary nitrogen atoms [N(32), N(36)] and phenoxido oxygen atoms [O(24)], one phenoxido oxygen atom O(24)^a of a second ligand together with O(1) of μ_4-CO_3^{2-}. The basal plane is constituted by O (24), N(32), N(36) and O(24)^a atoms. The N(1) atom of the acetonitrile molecule and O(1) atom of μ_4-CO_3^{2-} occupy the two axial positions. The Ni(2)–O(24)^a bond of 2.072(5) Å is shorter than the Ni–O(24) bond of 2.105(5) Å. Deviations of the coordinating atoms O(24), N(32), N (36) and O(24)^a from the least squares mean plane through them are 0.144(5), −0.130(7), 0.118(7), and −0.132(5) Å, respectively, and that of the Ni(2) atom from the same plane is 0.076(1) Å towards the axially coordinated N(1) atom. The Ni-N bonds fall in the range of 2.082(6)–2.125(9) Å. The bond with N(1) of acetonitrile is slightly longer than O(1) of bridging carbonato ligand in axial position with bridging angle, 178.3(3)°. In the structure, there are three hydrogen bonds which is shown in Fig. S2, N(32) to O(10), N(36) to Cl(1) and N (18) to O(52) with dimensions H(32)…O(10) 2.12 Å, H(36)…Cl(1) 2.40 Å, H(18)…O(52) 2.24 Å; N(32)…O(10) 3.059(9) Å, N(36)…Cl(1) 3.349(8) Å, N(18)…O(52) 3.141(13) Å and N(32)–H(32)…O(10) 159°, N(36)–H(36)…Cl(1) 163°, N(18)–H18…O(52) 153° respectively. Selected bond lengths and angles are summarized in Table S1.

Usually flack parameter gives the idea of absolute configuration in any chiral crystal. In case of complex 1, the value is 0.01(3) which indicates that enantiomeric purity of single crystal. The employment of ligands with a prochiral center in coordination chemistry generates chiral center in the final complex. The presence of chiral centers in the molecule induces the phenomenon of chirality transfer, which produces structures with predetermined supramolecular chirality that can be observed at different levels. In our case, the two N-donors of the Schiff base are bonded to three different groups (Scheme 2) and after coordination to the metallic cation become chiral centers which can have R or S configurations. The reaction that allows to the syntheses of HL is not selective and contains two prochiral N atoms, and thus, the starting ligand should be a racemic mixture of the (RR), (SS), (RS) and (SR) enantiomers. Noteworthy, it is surprising that among the four possible configurations (there is no steric impediment to change the H and methyl positions), the clusters of **1** are enantiomerically pure (RR) or (SS) isomers, related between them by reflection planes in the network.

This chirality is also transmitted to the Ni centers which have 6 different ligating atoms around them (which meant that are

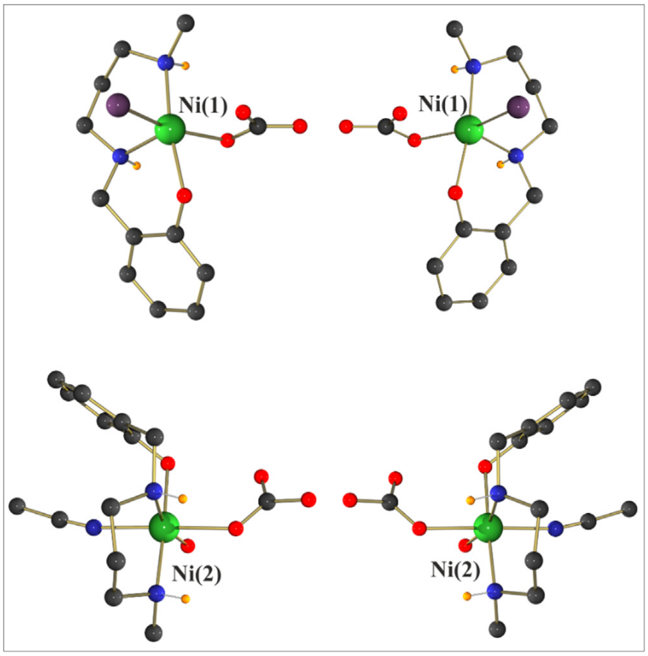

Fig. 2. Left, coordination sphere of Ni(1) and Ni(2) for the (RR)-L$^-$ ligand, and right, coordination sphere of Ni(1) and Ni(2) for the (SS)-L$^-$ ligand. The atom in orange show the H atoms coordinated to the N chiral centers. (For interpretation of the references to colour in this figure legend, the reader is referred to the web version of this article.)

automatically chiral centers). Fig. 2 represents the coordination spheres of Ni(1) for (RR) molecules and Ni(1) for (SS) molecules showing that they are not superimposable. The same is true for the coordination spheres of Ni(2).

Among the reported carbonato bridged complexes, the majority contain Cu(II) and Zn(II) ions in homonuclear and 3d(Cu, Ni, Zn)-4f ions in heteronuclear structures. Quite a few carbonato bridged Ni(II) complexes are also reported and the nuclearity of these complexes varies from Ni_2 to Ni_{12}. Of these structures, only two are tetranuclear and the bridging mode of carbonate in these two are: $\{\eta^1:\eta^1:\eta^2\text{-}\mu_4\}$ and $\{\eta^2:\eta^2\text{-}\mu_4\}$ [29,42]. Thus, the present complex is only the third example of carbonato-bridged tetranuclear Ni(II) complex and a new coordination mode of carbonate ($\mu_4\text{-}\kappa^2:\kappa^2:\eta^1:\eta^1$) to Ni(II) is identified in it.

3.4. Magnetic properties

The $\chi_M T$ product plotted as $\chi_M T$ *vs.* T for complex **1** is represented in Fig. 3 in the temperature range 2–300 K. The magnetic behaviour of the carbonate bridge presents different type of interactions depending on the coordination mode, and has been widely studied for many paramagnetic metallic centers [43–45]. The bridging modes which are present in complex **1** are shown in Fig. 4. The experimental χT value of 4.03 $cm^3 \cdot K \cdot mol^{-1}$ at room temperature, agrees perfectly with the expected value of four non interacting Ni(II) cations. The curve decays with lowering of temperature, reaching $S = 0$ at low temperature. This behaviour is characteristic of a carbonate bridged paramagnetic centers with a global antiferromagnetic coupling.

The plot of χ_M *vs.* T is represented in Fig. 3, inset which has a value of 0.013 $cm^3 \cdot mol^{-1}$ at room temperature and increases continuously when the temperature decreases reaching a maximum value of 0.071 $cm^3 \cdot mol^{-1}$ at 13 K and decreasing again to a final value of 0.028 $cm^3 \cdot mol^{-1}$ at 2 K. This behaviour with a maximum in the χ_M *vs.* T curve, confirms the global antiferromagnetic behaviour and the $S = 0$ ground state of complex **1**.

From the structural data we realized that there are four main, clearly different superexchange pathways: the interaction between Ni(1) and Ni(2) which is mediated by one oxo donor with a large Ni–O–Ni bond angle of 175.2°, two interactions between Ni(1) and Ni(2) (and symmetry related ones) with a Ni–O–Ni bond angle of 140.5°, two syn-anti carbonato bridges and finally the Ni(2)–Ni(2)′ interaction mediated by phenoxo bridges with Ni–O–Ni bond angles of 98.2°. On the basis of these interactions, the coupling scheme for **1** is depicted in Fig. 5 and the derived isotropic spin-Hamiltonian to fit the magnetic behavior of the complex using the PHI software [46] is:

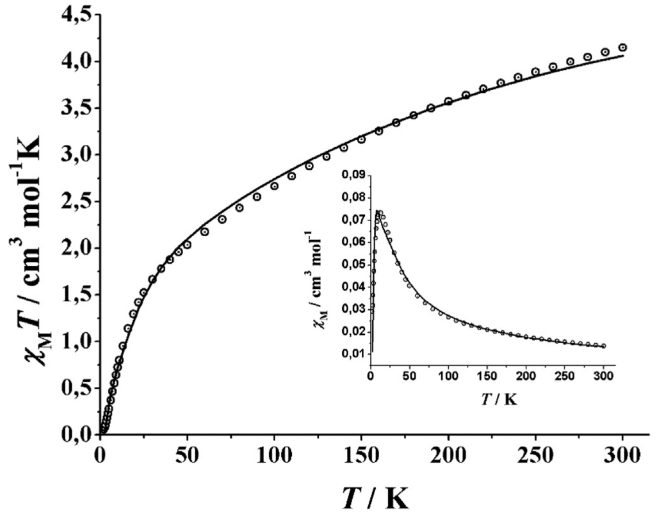

Fig. 3. $\chi_M T$ *vs.* T for complex **1**. Inset, χ_M *vs.* T representation which confirms the overall antiferromagnetic behaviour. Solid lines represent the best fits.

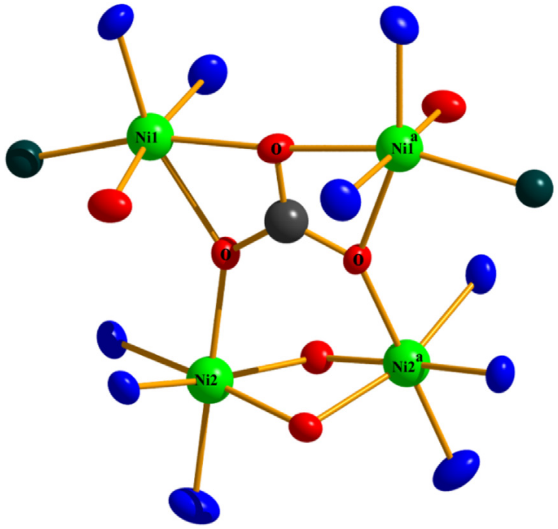

Fig. 4. Environments of Ni(II) ions in complex **1** with different bridging modes (phenoxido, $\mu_4\text{-}\kappa^2:\kappa^2:\eta^1:\eta^1$-carbonato).

$$H = -2J_1(\hat{S}_{Ni1} \cdot \hat{S}_{Ni1'}) - 2J_2(\hat{S}_{Ni1} \cdot \hat{S}_{Ni2} + \hat{S}_{Ni1'} \cdot \hat{S}_{Ni2'}) - 2J_3(\hat{S}_{Ni1} \cdot \hat{S}_{Ni2'} + \hat{S}_{Ni1'} \cdot \hat{S}_{Ni2}) - 2J_4(\hat{S}_{Ni2} \cdot \hat{S}_{Ni2'})$$

The fit yields in the values of $J_1 = -60.32\ cm^{-1}$, $J_2 = -19.52\ cm^{-1}$, $J_3 = 2.6\ cm^{-1}$ and $J_4 = 3.3\ cm^{-1}$. The g value is 2.3. As should be expected, the stronger antiferromagnetic interaction corresponds to the larger Ni–O–Ni bond angle (J_1), a lower but also strong interaction to the two Ni-O-Ni bond angles (J_2). The *syn-anti* interactions mediated by the carbonato bridge are a poor superexchange pathway (J_3) and the J_4 value is characteristic of phenoxo bridges with bond angles close to the ferro-antiferromagnetic border. Despite the weak ferromagnetic character of J_3 and J_4 very strong

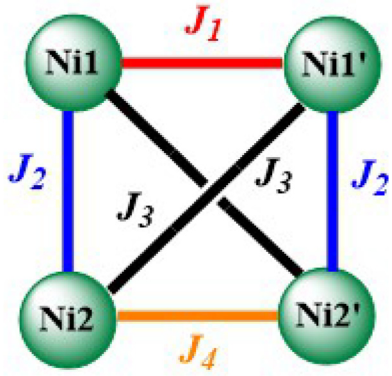

Fig. 5. Coupling scheme for complex **1** with two antiferromagnetic exchange pathways (J_1 and J_2) and two ferromagnetic pathways (J_3 and J_4).

antiferromagnetic interaction through Ni(1) and Ni(1′) with an angle of 175.2° (J_1) and the also antiferromagnetic coupling between Ni(1)–Ni(2) and Ni(1′)–Ni(2′) (J_2) dominate the overall couplings.

As the magnitude of J_3 and J_4 are very small compared to that of J_1 and J_2, a second fit was tried using only J_1 and J_2. However, this approach resulted in a worse fitting of the curve because, the product was not diamagnetic below 10 K ($\chi_M T \sim 1\ \mathrm{cm^3{\cdot}K{\cdot}mol^{-1}}$), and therefore J_3 and J_4 cannot be neglected.

4. Conclusion

In this paper, we have shown the formation of a tetranuclear Ni(II) complex by spontaneous absorption of aerial CO_2 and thereby *in situ* generation of carbonate ligand. The novelty of the work is in that a simple N_2O donor reduced Schiff base ligand is found to be effective as ancillary ligand for the atmospheric CO_2 fixation, which is very rare in the literature and a new bridging mode (μ_4-κ^2:κ^2:η^1:η^1) of CO_3^{2-} to Ni(II) has been identified in complex **1**. This bridging mode of the central carbonate anion along with a diphenoxido bridge affords a unique connectivity between the paramagnetic octahedral Ni(II) ions in the complex, which plays a crucial role in the observed overall antiferromagnetic coupling. The analysis of magnetic data suggests that the carbonato oxygen atoms mediate strong antiferromagnetic coupling as the bridging angle is very wide (175.2°, 140.4°) whereas weak ferromagnetic coupling occurs through phenoxido bridge as the bridging angle is much smaller (98.2°) and also via the *syn-anti* carbonate bridge. Further studies are going on to isolate some more complexes of this type with various metal ions in order to understand the driving forces for atmospheric CO_2 fixation during the preparation of such complexes and to investigate their magnetic properties.

Acknowledgment

A. G. thanks the DST-FIST funded single crystal X-ray diffractometer facility at the department of chemistry, University of Calcutta for providing the single crystal X-ray diffractometer facility. A.G. also thanks University Grants Commission (UGC), New Delhi for funding the CAS-V, Department of Chemistry, University of Calcutta. J. M. thanks the Ministerio de Economía y Competitividad, Project CTQ2015-63614-P for funding.

Appendix A. Supplementary data

Supplementary data to this article can be found online at https://doi.org/10.1016/j.ica.2019.119175.

References

[1] G.A. Olah, G.S. Prakash, A. Goeppert, J. Am. Chem. Soc. 133 (2011) 12881.
[2] M. Mikkelsen, M. Jørgensen, F.C. Krebs, Energy Environ. Sci. 3 (2010) 43.
[3] M. Cokoja, C. Bruckmeier, B. Rieger, W.A. Herrmann, F.E. Kühn, Angew. Chem. Int. Ed. 50 (2011) 8510.
[4] A.M. Appel, J.E. Bercaw, A.B. Bocarsly, H. Dobbek, D.L. DuBois, M. Dupuis, J.G. Ferry, E. Fujita, R. Hille, P.J. Kenis, C.A. Kerfeld, Chem. Rev. 113 (2013) 6621.
[5] Z. Zhang, Z.Z. Yao, S. Xiang, B. Chen, Energy Environ. Sci. 7 (2014) 2868.
[6] N.J. English, M.M. El-Hendawy, D.A. Mooney, J.M.D. MacElroy, Coord. Chem. Rev. 269 (2014) 85.
[7] A. Sanna, M. Uibu, G. Caramanna, R. Kuusik, M.M. Maroto-Valer, Chem. Soc. Rev. 43 (2014) 8049.
[8] (a) R.L. Paddock, S.T. Nguyen, J. Am. Chem. Soc. 123 (2001) 11498;
(b) B. Das, M. Bhadbhade, A. Thapper, C.D. Ling, S.B. Colbran, Dalton Trans. 48 (2019) 3576.
[9] K. Sołtys-Brzostek, M. Terlecki, K. Sokołowski, J. Lewiński, Coord. Chem. Rev. 334 (2017) 199.
[10] A. Sigel, H. Sigel, R. Sigel, John Wiley & Sons 12 (2008).
[11] M. Sola, A. Lledos, M. Duran, J. Bertran, J. Am. Chem. Soc. 114 (1992) 869.
[12] L. Cronin, S.P. Foxon, P.J. Lusby, P.H. Walton, J. Biol. Inorg. Chem. 6 (2001) 367.
[13] (a) M. Sarkar, G. Aromí, J. Cano, V. Bertolasi, D. Ray, Chem. Eur. J. 16 (2010) 13825;
(b) A. Das, S. Goswami, R. Sen, A. Ghosh, Inorg chem. 58 (2019) 5787;
(c) M.C. Majee, S.M.T. Abtab, D. Mondal, M. Maity, M. Weselski, M. Witwicki, A. Bieńko, M. Antkowiak, G. Kamieniarz, M. Chaudhury, Dalton Trans. 47 (2018) 3425.
[14] T.N. Hooper, R. Inglis, M.A. Palacios, G.S. Nichol, M.B. Pitak, S.J. Coles, G. Lorusso, M. Evangelisti, E.K. Brechin, Chem. Commun. 50 (2014) 3498.
[15] (a) L. Jiang, Y. Liu, X. Liu, J. Tian, S. Yan, Dalton Trans. 46 (2017) 12558;
(b) H. Tian, L. Zhao, J. Tang, Cryst. Growth Des. 18 (2018) 1173.
[16] J. Goura, E. Colacio, J.M. Herrera, E.A. Suturina, I. Kuprov, Y. Lan, W. Wernsdorfer, V. Chandrasekhar, Chem. Eur. J. 23 (2017) 16621.
[17] J.C. Anderson, A.J. Blake, R.B. Moreno, G. Raynel, J. van Slageren, Dalton Trans. 42 (2009) 9153.
[18] S.S. Massoud, F.R. Louka, M.A. Al-Hasan, R. Vicente, F.A. Mautner, New J. chem. 39 (2015) 5944.
[19] H. Harada, M. Kodera, G. Vuckovic, N. Matsumoto, S. Kida, Inorg. Chem. 30 (1991) 1190.
[20] A.A. Lozano, M. Sáez, J. Pérez, L. García, L. Lezama, T. Rojo, G. López, G. García, M.D. Santana, Dalton Trans. 32 (2006) 3906.
[21] P.K. Nanda, M. Bera, G. Aromí, D. Ray, Polyhedron 25 (2006) 2791.
[22] R. McLellan, J. Rezé, S.M. Taylor, R.D. McIntosh, E.K. Brechin, S.J. Dalgarno, Chem. Commun. 50 (2014) 2202.
[23] D. Sun, G.G. Luo, N. Zhang, R.B. Huang, L.S. Zheng, Chem. Commun. 47 (2011) 1461.
[24] K. Xiong, F. Jiang, Y. Gai, Z. He, D. Yuan, L. Chen, K. Su, M. Hong, Cryst. Growth Des. 12 (2012) 3335.
[25] A.N. Georgopoulou, C.P. Raptopoulou, V. Psycharis, R. Ballesteros, B. Abarca, A.K. Boudalis, Inorg. Chem. 48 (2009) 3167.
[26] G.A. Craig, O. Roubeau, J. Ribas-Ariño, S.J. Teat, G. Aromí, Polyhedron 52 (2013) 1369.
[27] M. Pait, A. Bauzá, A. Frontera, E. Colacio, D. Ray, Inorg. Chem. 54 (2015) 4709.
[28] A.K. Ghosh, M. Pait, M. Shatruk, V. Bertolasi, D. Ray, Dalton Trans. 43 (2014) 1970.
[29] M. Fondo, N. Ocampo, A.M. García-Deibe, R. Vicente, M. Corbella, M.R. Bermejo, J. Sanmartín, Inorg. Chem. 45 (2006) 255.
[30] P. Mukherjee, M.G.B. Drew, M. Estrader, A. Ghosh, Inorg. Chem. 47 (2008) 7784.
[31] C. Biswas, M.G.B. Drew, A. Ghosh, Inorg. Chem. 47 (2008) 4513.
[32] M. Mondal, S. Giri, P.M. Guha, A. Ghosh, Dalton Trans. 46 (2017) 697.
[33] G.M. Sheldrick, Acta Crystallogr., Sect. C 71 (2015) 3.
[34] G.M. Sheldrick, Program for empirical absorption correction of area detector data, SADABS (1996).
[35] I. Usón, G.M. Sheldrick, Acta Crystallogr. Sect. D 74 (2018) 106.
[36] A. Biswas, L.K. Das, M.G.B. Drew, G. Aromí, P. Gamez, A. Ghosh, Inorg. Chem. 51 (2012) 7993.
[37] M. Mondal, P.M. Guha, S. Giri, A. Ghosh, J. Mol. Catal. A: Chem. 424 (2016) 54.
[38] A. Biswas, M.G.B. Drew, J. Ribas, C. Diaz, A. Ghosh, Eur. J. Inorg. Chem. 15 (2011) 2405.
[39] M. Mondal, M. Chakraborty, M.G.B. Drew, A. Ghosh, Magnetochemistry 4 (2018) 51.
[40] A. Biswas, M.G.B. Drew, A. Ghosh, Polyhedron 29 (2010) 1029.
[41] (a) X.L. Tang, W.H. Wang, W. Dou, J. Jiang, W.S. Liu, W.W. Qin, G.L. Zhang, K.B. Yu, L.M. Zheng, Angew. Chem., Int. Ed. 48 (2009) 3499;
(b) P. Mateus, R. Delgado, F. Lloret, J. Cano, P. Brandão, V. Félix, Chem. Eur. J. 17 (2011) 11193.
[42] M. Fondo, N. Ocampo, A.M. García-Deibe, E. Ruíz, J. Tercero, J. Sanmartín, Inorg. Chem. 48 (2009) 9861.
[43] A. Escuer, R. Vicente, S.B. Kumar, X. Solans, M.B.A. Caneschi, Inorg. Chem. 35 (1996) 3094.
[44] A. Escuer, E. Peñalba, R. Vicente, X. Solans, Dalton Trans. 4 (1997) 2315.
[45] A. Escuer, M. Fallah, S. Kumar, F. Vicente, Polyhedron 18 (1999) 377.
[46] N.F. Chilton, R.P. Anderson, L.D. Turner, A. Soncini, K.S. Murray, J. Comput. Chem. 34 (2013) 1164.